

Supporting Information:

**Hollow MoS₂-Supported MAPbI₃ Composites for effective
photocatalytic hydrogen evolution**

Jiaqi He[†], Xiang Li[†], Tiantian Zhang, Qiulin Li, Yongbing Lou, Jinxi Chen^{*}

School of Chemistry and Chemical Engineering, Southeast University, Nanjing
211189, PR China.

* Corresponding author.

E-mail: chenjinxi@seu.edu.cn

Chemicals:

All reagents were used without any purification. PbI_2 (Lead(II) Iodide, 99%, Aldrich), hydroiodic acid (HI, 57 wt.% in water, Aladdin), methylamine (CH_3NH_2 , 30 wt.% in absolute ethanol, Aladdin), hypophosphorous acid (H_3PO_2 , 50wt% in water, Aladdin), Manganese Carbonate (MnCO_3 , Aladdin), L-cysteine ($\text{C}_3\text{H}_7\text{NO}_2\text{S}$, Aladdin), Sodium molybdate ($\text{Na}_2\text{MoO}_4 \cdot 2\text{H}_2\text{O}$), Ethyl acetate ($\text{C}_4\text{H}_8\text{O}_2$, 99.8%, Sinopharm)

Synthesis of MAI:

Under ice water bath, 20 mL of HI solution and 45 mL of CH_3NH_2 ethanolic solution were added to the round-bottomed flask, and stirring was continued for 2 hours; the solution was then transferred to a rotary evaporator and evaporated to dryness at 60 °C. The obtained solid powder was dissolved in anhydrous ethanol and recrystallized from anhydrous ether. This process was repeated 3 times to obtain a white powder. Dry in a vacuum oven at 60 °C for ten hours to obtain a white MAI powder.

Characterizations

The phase structure of the material can be obtained by analyzing the X-ray diffraction pattern ($\text{Cu K}\alpha$ ($\lambda = 0.15406 \text{ nm}$)). The Zeta potential of H-MoS_2 and MAPbI_3 was measured using a multi-angle particle size potential analyzer (Nanobrook Omni). Sample preparation method: the sample is dispersed in HI solution through ultrasonic treatment, and then the suspension is put in the sample pool for detection. FEI Inspect F50 scanning electron microscope was used to characterize the morphology and element distribution of the samples; TEM and HRTEM images of the material were obtained by FEI G2 20 transmission electron microscope with an accelerating voltage of 200 eV. The absorption spectra of the materials were obtained with an ultraviolet-visible (UV-vis) spectrophotometer (UV2700), and the photoluminescence (PL) was obtained on a Fluoromax-4 fluorescence spectrometer (Horiba), and fit the mean life using a second-order function. X-ray photoelectron spectroscopy (XPS) was used to characterize the chemical state information of the element surface, and the carbon signal at 284.8 eV was used for nuclear correction. Gaussian fitting was performed on the obtained energy spectral images using the corresponding software.

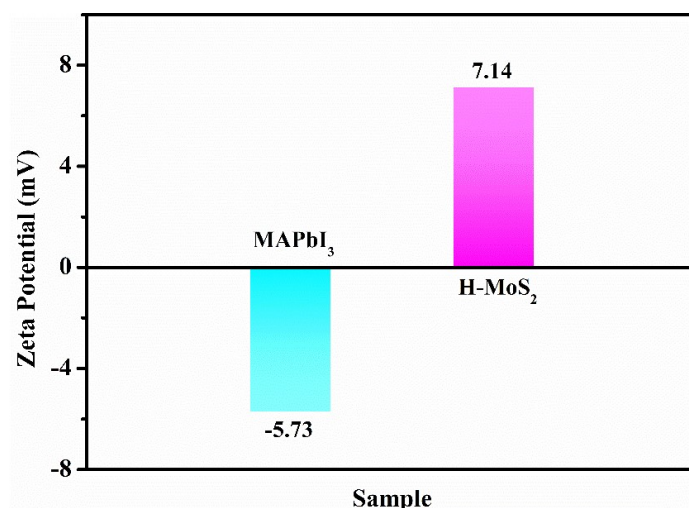


Figure S1. Zeta potentials of MAPbI_3 and H-MoS_2 .

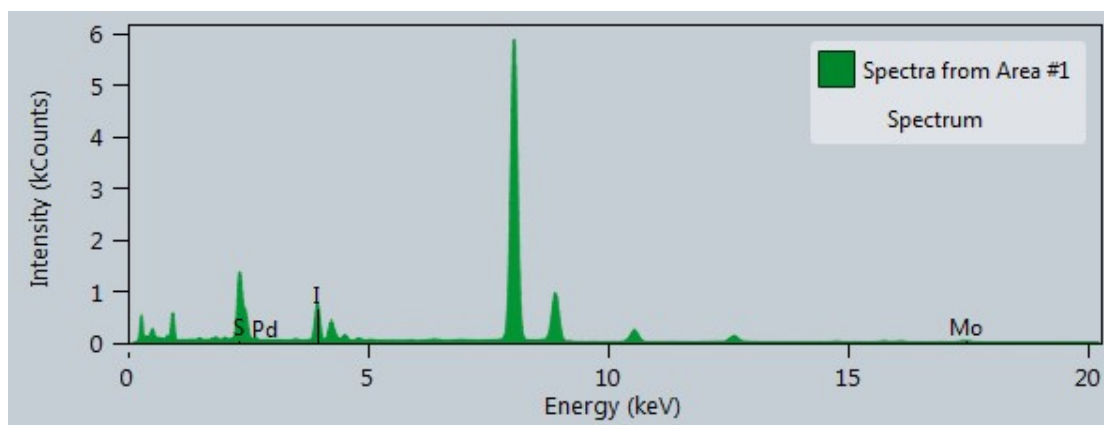


Figure S2. EDS analysis spectra

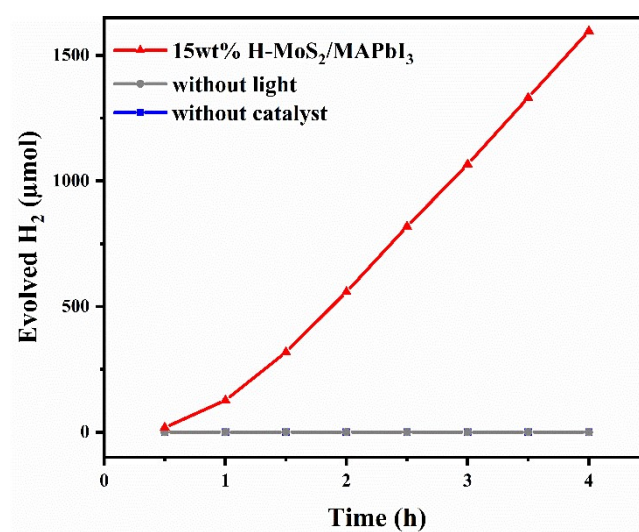


Figure S3. Comparison of H_2 evolution activities of 15wt%H-MoS₂/MAPbI₃, without light irradiation and without photocatalyst.

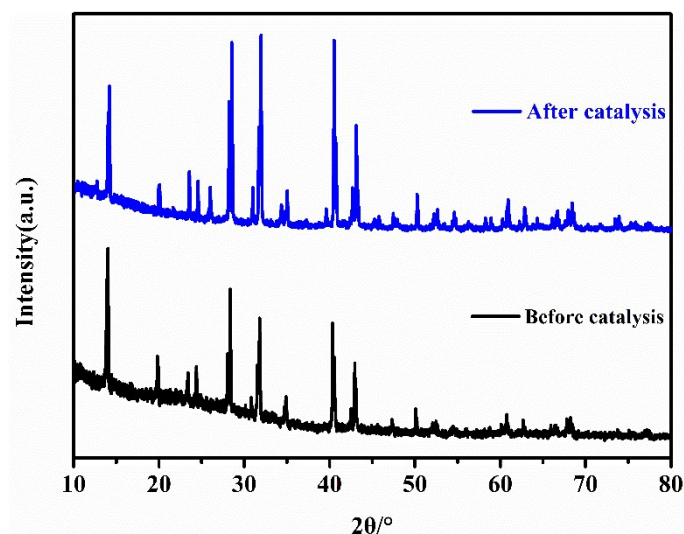


Figure S4. (a) XRD patterns 15% H-MoS₂/MAPbI₃ before and after catalysis.

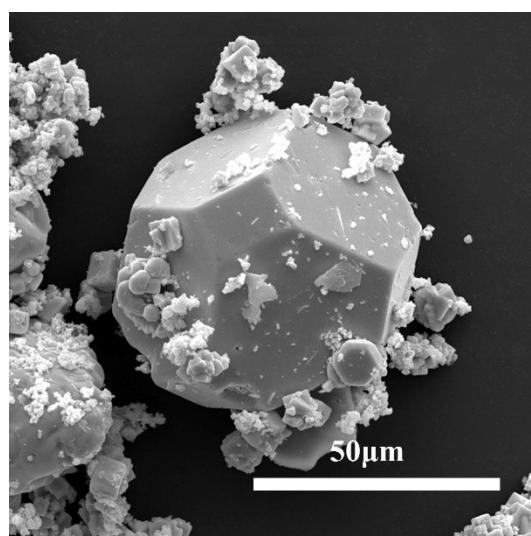


Figure S5. SEM images of 15% H-MoS₂/MAPbI₃ after catalysis.

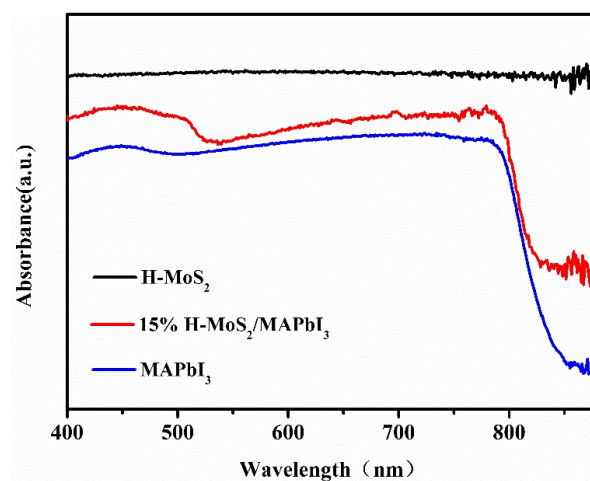


Figure S6. UV-vis absorption spectra of MoS₂, MAPbI₃ and 15% MoS₂/MAPbI₃.

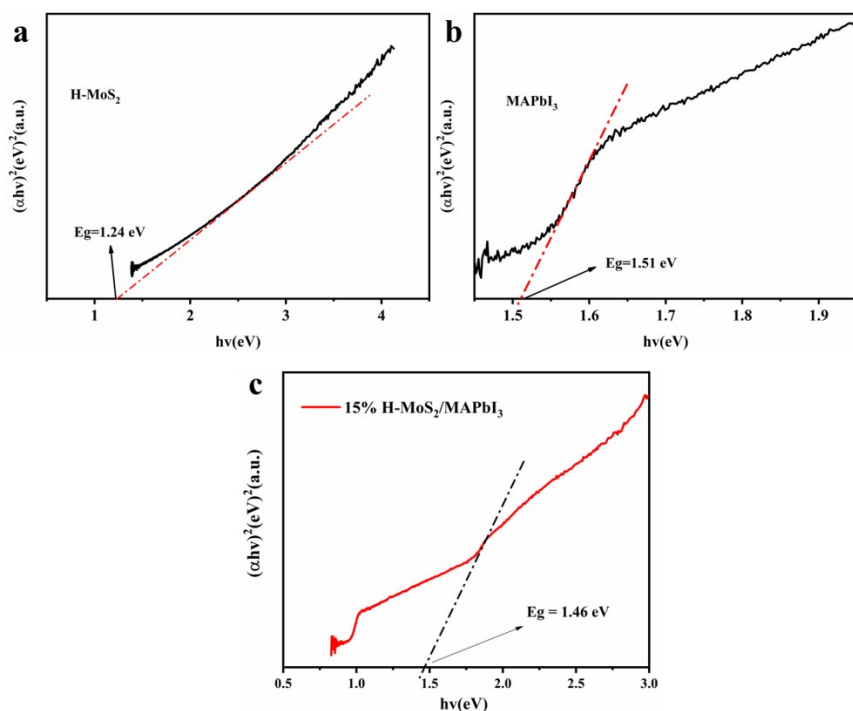


Figure S7. Band gap energy (E_g) of H-MoS_2 , MAPbI_3 and $\text{H-MoS}_2/\text{MAPbI}_3$ calculated by Tauc plot absorption spectroscopy.

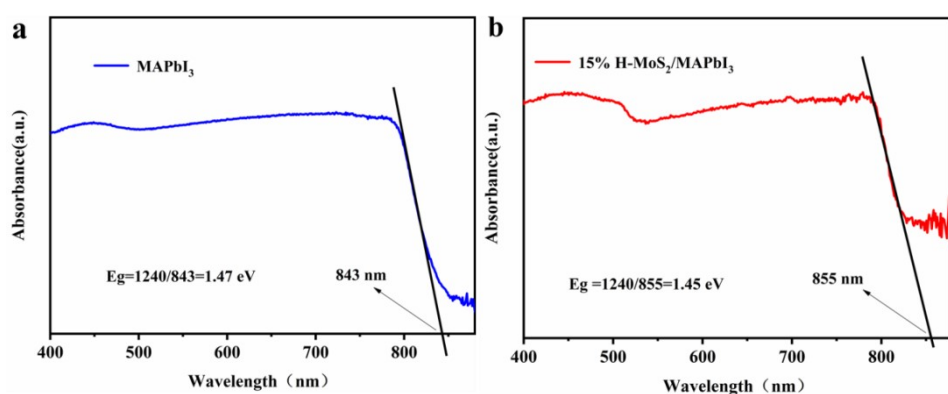


Figure S8. Band gap energy (E_g) of MAPbI_3 and $\text{H-MoS}_2/\text{MAPbI}_3$ calculated by tangent method.

Table S1. Comparison of H_2 evolution over reported MAPbI_3 in photocatalytic HI splitting system.

Materials	Light source (λ in nm)	H_2 activity ($\mu\text{mol}\cdot\text{h}^{-1}$)	Ref
Pure MAPbI_3	300 W Xe lamp ($\lambda \geq 420$ nm)	1.53	This work
$\text{H-MoS}_2/\text{MAPbI}_3$	300 W Xe lamp ($\lambda \geq 420$ nm)	399	This work

MAPbI ₃ /Pt	300 W Xe lamp ($\lambda \geq 420$ nm)	15.1	This work
MAPbI ₃ /Pt	100W solar simulat ($\lambda > 475$ nm)	0.57	1
MAPbI ₃ /rGO	300 W Xe lamp ($\lambda \geq 420$ nm)	93.9	2
MA ₃ Bi ₂ I ₉	300 W Xe lamp ($\lambda \geq 420$ nm)	16.9	3
MAPbI ₃ /Ni ₃ C	300 W Xe lamp ($\lambda \geq 420$ nm)	236	4
MAPb(I _{1-x} Br _x) ₃	300 W Xe lamp ($\lambda \geq 420$ nm)	147	5
MAPbI ₃ /CoP	150 W Xe lamp ($\lambda \geq 420$ nm)	236.2	6
MAPbI ₃ /Pt/TiO ₂	300 W Xe lamp ($\lambda \geq 420$ nm)	529.3	7
MAPbI ₃ /BP	300 W Xe lamp ($\lambda \geq 420$ nm)	374	8

1. S. Park, W. J. Chang, C. W. Lee, S. Park, H.-Y. Ahn and K. T. Nam, *Nature Energy*, 2016, **2**, 16185.
2. Y. Wu, P. Wang, X. Zhu, Q. Zhang, Z. Wang, Y. Liu, G. Zou, Y. Dai, M.-H. Whangbo and B. Huang, *Advanced Materials*, 2018, **30**, 1704342.
3. Y. Guo, G. Liu, Z. Li, Y. Lou, J. Chen and Y. Zhao, *ACS Sustainable Chemistry & Engineering*, 2019, **7**, 15080-15085.
4. Z. Zhao, J. Wu, Y.-Z. Zheng, N. Li, X. Li and X. Tao, *ACS Catalysis*, 2019, **9**, 8144-8152.
5. Z. Zhao, J. Wu, Y.-Z. Zheng, N. Li, X. Li, Z. Ye, S. Lu, X. Tao and C. Chen, *Applied Catalysis B: Environmental*, 2019, **253**, 41-48.
6. C. Cai, Y. Teng, J.-H. Wu, J.-Y. Li, H.-Y. Chen, J.-H. Chen and D.-B. Kuang, *Advanced Functional Materials*, 2020, **30**, 2001478.
7. X. Wang, H. Wang, H. Zhang, W. Yu, X. Wang, Y. Zhao, X. Zong and C. Li, *ACS Energy Letters*, 2018, **3**, 1159-1164.
8. R. Li, X. Li, J. Wu, X. Lv, Y.-Z. Zheng, Z. Zhao, X. Ding, X. Tao and J.-F. Chen, *Applied Catalysis B: Environmental*, 2019, **259**, 118075.